

A complete active space valence bond method with nonorthogonal orbitals

Kimihiko Hirao, Haruyuki Nakano, and Kenichi Nakayama

Department of Applied Chemistry, Graduate School of Engineering, The University of Tokyo, Tokyo, Japan 113

(Received 21 May 1997; accepted 10 September 1997)

A complete active space self-consistent field (SCF) wave function is transformed into a valence bond type representation built from nonorthogonal orbitals, each strongly localized on a single atom. Nonorthogonal complete active space SCF orbitals are constructed by Ruedenberg's projected localization procedure so that they have maximal overlaps with the corresponding minimum basis set of atomic orbitals of the free-atoms. The valence bond structures which are composed of such nonorthogonal quasiatomic orbitals constitute the wave function closest to the concept of the oldest and most simple valence bond method. The method is applied to benzene, butadiene, hydrogen, and methane molecules and compared to the previously proposed complete active space valence bond approach with orthogonal orbitals. The results demonstrate the validity of the method as a powerful tool for describing the electronic structure of various molecules. © 1997 American Institute of Physics. [S0021-9606(97)01647-4]

I. INTRODUCTION

In a previous publication,¹ a method was outlined for determining the complete active space valence bond (CASVB) wave functions. They are obtained simply by transforming a canonical complete active space self-consistent field (CASSCF) function² and are readily interpreted in terms of the well-known classical valence bond (VB) resonance structures. The method is applied to the ground and excited states of benzene, butadiene, and the ground state of methane. CASVB affords a clear view of the wave functions for the various states and forms a useful bridge from molecular orbital (MO) theory to the familiar concepts of chemists. CASVB provides greater insight than delocalized MO-based methods, yet the methods are complementary, each one providing different perspectives that arise from identical total densities and total energies.

The CASSCF (Ref. 2) or full optimized reaction space (FORS) (Ref. 3) method is an attempt to generalize the Hartree-Fock (HF) model to situations where the state-specific nondynamical correlation is important, while keeping the conceptual simplicity of the HF model as much as possible. It is size-consistent and the wave function is invariant to linear transformations among active orbitals. Although CASSCF does not include dynamical correlation, it can easily be taken into account by a CASSCF-based perturbation theory, such as CASPT2 by Roos *et al.*⁴ and our multireference Møller-Plesset theory (MRMP).⁵

In the previous treatment, we determined the atomiclike localized MO's (LMO's) by a unitary transformation with Boy's localization procedure.⁶ LMO's obtained in this manner nearly always turn out to be well localized on a single atomic center. Each LMO resembles the atomiclike function. Although very atomic in nature, LMO's are still MO's and therefore these LMO's are orthogonal. The localized MO's possess small tails on the other atoms in order to maintain their orthogonality to each other. The classical VB function is a linear combination of configuration state functions of VB

type constructed with tailless orbitals, each purely localized on a single center. Thus, the less atomiclike the localized orbitals become, the greater the difference will be between this approach and a conventional VB calculation. A CASVB representation with orthogonal LMO's tends to introduce a somewhat greater degree of mixing of ionic structures, even for states having largely covalent character. The requirement for ionic structures arises mainly from the orthogonality constraints. Ohanessian and Hiberty⁷ studied critically the use of orthogonalized atomic orbitals (AO's) in VB type wave functions and concluded that VB with orthogonal orbitals places a higher weight on ionic structures than when nonorthogonal orbitals are used.

The invariance of the CASSCF (FORS) wave function to linear transformations among active orbitals has inspired a number of localization schemes,^{8,9} analogous to those used for single determinantal SCF wave functions.^{6,10} Ruedenberg *et al.*⁸ have shown that CASSCF active orbitals can be chosen as being so strongly localized that they are almost identical with the minimal basis set of the SCF AO's of the free atoms. This involves the projection of the canonical FORS MO onto the atomic basis, followed by symmetric orthogonalization of the resulting projections. They call the projected localized FORS MO's as the "atom-adapted minimum FORS MO's." McDouall and Robb⁹ have proposed an intrinsic localization procedure for active CASSCF orbitals. The CASSCF wave function obtained using these localized active orbitals corresponds to a full VB calculations where the VB structures are built from orthogonal quasiatomic orbitals.

Nonorthogonal orbitals have also been used to express the CASSCF wave functions in terms of the VB structures. In 1987, McDouall and Robb¹¹ have shown the transformation of the CASSCF wave function to the spin-coupled (SC) VB wave function of Gerratt *et al.*¹² The orthogonal localized orbitals obtained by the intrinsic localization procedure⁹ are transformed to nonorthogonal orbitals by orbital rotations among CASSCF active orbitals. Thorsteinsson *et al.*¹³ also

investigated the transformations of CASSCF functions to modern VB representations (they also call it CASVB). They examined transformations for which the total wave function is dominated by covalent structures built from a common product of nonorthogonal orbitals.

Any full CI wave function is invariant under linear transformations of the defining orbitals, and we may choose to transform the orbitals to a nonorthogonal set that is similar to those which arise in classical VB theory. The method we develop in this paper can be defined as a CASVB wave function built from nonorthogonal orbitals each strongly localized on a single atom. The nonorthogonal LMO's are determined following to Ruedenberg's suggestion so that they have the maximal overlap with the minimal basis set of AO's of the free atoms.⁸ The VB structures composed of such nonorthogonal quasiautomatic orbitals are expected to constitute wave functions that are closest to the concept of the oldest and most simple VB method.

In Sec. II we will describe in more detail how to obtain the CASVB functions with nonorthogonal orbitals. Applications to benzene, butadiene, hydrogen, and methane molecules are discussed in Sec. III. A summary is given in the final section.

II. CASVB METHOD WITH NONORTHOGONAL ORBITALS

The details of the CASVB method with orthogonal orbitals have been given in the previous publication.¹ Here we will give a brief survey of the main features. We first carry out a standard CASSCF calculation. The CASSCF wave function is invariant against unitary transformations among active orbitals. Making use of this arbitrariness, we can construct LMO's. The LMO's are nearly always well localized on a single atomic center with small localization tails onto the neighboring atoms. Then the bonded functions with the Rumer spin eigenfunctions based on these LMO's are constructed and a full CI is performed within the active space spanned by the bonded functions. That is, the CASSCF function is projected onto the space spanned by the VB functions. The total energies and total densities are, of course, identical to those of the canonical CASSCF. The Rumer spin functions are linearly independent but nonorthogonal to each other. These are specified by the branching diagram or the standard Young tableaux. There is a one-to-one correspondence between the spin couplings specified by the standard Young tableaux or the branching diagram symbols and the covalent VB structures.

The relative weight (the occupation number) n_I for the VB structure I is defined as

$$n_I = C_I \sum_J S_{IJ} C_J,$$

where the sum goes over all the VB structures. The C_I is the coefficient of the VB structure I and S_{IJ} is the overlap integral between structures I and J . The n_I 's add up to 1,

$$\sum_I n_I = 1.$$

The n_I 's give an estimate of the importance of the VB structure. This is the outline of the CASVB method with orthogonal LMO's.

Now let us consider the case of nonorthogonal LMO's. What is a criterion for choosing a nonorthogonal set? It is desirable to have some well-defined criterion for the transformation of the CASSCF orbitals to LMO's that are similar to those which arise in VB theory. The canonical MO method puts electrons into orthogonal delocalized MO's while the VB method puts electrons into nonorthogonal AO's. Thus, we will employ Ruedenberg's procedure of projected localized MO's (Ref. 8) and obtain quasiautomatic CASSCF MO's which have maximal overlaps with the minimum basis of AO's of the free atoms.

Let P be the projection operator constructed by CASSCF active orbitals φ_i ,

$$P = \sum_i |\varphi_i\rangle\langle\varphi_i|.$$

Consider a free-atom minimum basis set of AO's, χ_A , centered on a nucleus A . Diagonalizing

$$P|\chi_A\rangle\langle\chi_A|P,$$

and choosing the eigenvector with the largest eigenvalue gives the LMO, λ_A , which has the maximum overlap with χ_A . Similarly we can define $\lambda_B, \lambda_C, \dots$. The $\{\lambda_\mu\}$ obtained in this manner are nonorthogonal to each other. Ruedenberg⁸ orthogonalized these atom-adapted LMO's but we are willing to abandon the orthogonality requirements. A set of nonorthogonal atom-adapted CASSCF MO's is much closer to the minimal basis set of the free-atom SCF AO's than a set of orthogonal ones.

The exact form of the χ_A 's was not specified; they can be the minimum basis set of s , p , or d type AO's or they can be arbitrary independent hybrid AO's. We may also choose the floating functions that are not atom centered. The floating functions can introduce the polarization effect to the SCF atomic functions. Thus, an arbitrary nonorthogonal transformation is still undetermined on any one atom and we shall find several uses for this remaining freedom.

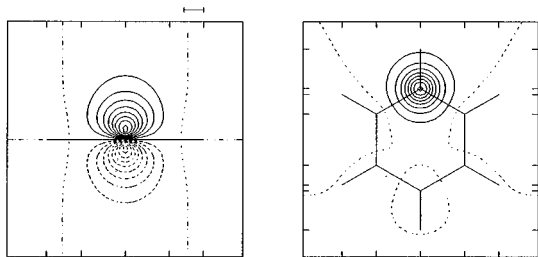
The full configuration space of all possible configurations which are generated by these quasiautomatic CASSCF MO's is identical with that of full CI space which is constructed from the canonical CASSCF MO's. Thus, we use $\{\lambda_\mu\}$ from which a CASVB wave function is constructed. To obtain the weights of the corresponding VB structures, we project a canonical CASSCF wave function onto a VB wave function. The projection does not modify the original wave function but simply reexpress it in the VB language. Let Ψ^{CASSCF} be a canonical CASSCF wave function

$$\Psi^{\text{CASSCF}} = \sum_i C_i \Phi_i^{\text{CASSCF}}, \quad \Phi_i^{\text{CASSCF}} \equiv \Phi_i^{\text{CASSCF}}(\{\varphi_i\}),$$

where Φ_i^{CASSCF} are the configuration state functions constructed by orthogonal orbitals $\{\varphi_i\}$ and C_i 's are the known full CI expansion coefficients. Similarly we can define the CASVB function in terms of bonded functions as

$$\Psi^{\text{CASVB}} = \sum_i A_i \Phi_i^{\text{CASVB}}, \quad \Phi_i^{\text{CASVB}} \equiv \Phi_i^{\text{CASVB}}(\{\lambda_i\}),$$

Orthogonal orbitals



Non-orthogonal orbitals

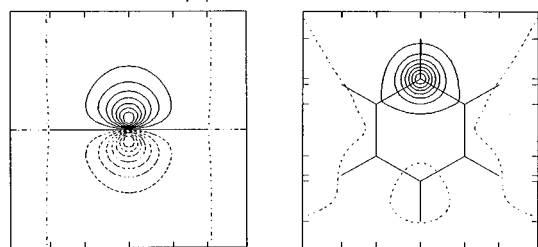


FIG. 1. One of the six equivalent orthogonal and nonorthogonal π orbitals of benzene. Contours are plotted in a σ_h mirror (perpendicular to the molecular plane) and plotted in the plane 0.3 Å above the σ_h plane.

where Φ_i^{CASVB} are bonded functions constructed by nonorthogonal LMO's $\{\lambda_i\}$, and A_i 's are the expansion coefficients to be determined. The total wave functions Ψ^{CASVB} and Ψ^{CASSCF} are the same except for their phase factor. Projecting Φ_i^{CASSCF} onto Ψ^{CASVB} and Ψ^{CASSCF} , we have

$$\sum_j \Omega_{ij} A_j = C_i \quad \text{with} \quad \Omega_{ij} = \langle \Phi_i^{\text{CASSCF}} | \Phi_j^{\text{CASVB}} \rangle.$$

The expansion coefficients $\{A_i\}$ are obtained by solving the above linear equations. This procedure only requires the calculation of one-electron overlap integrals Ω_{ij} .

III. RESULTS AND DISCUSSIONS

A. Benzene

To describe the electronic structure of benzene, we first carried out a standard CASSCF calculation using a basis set of double zeta plus polarization quality, $(3s2p1d/2s1p)$, taken from Dunning's correlation-consistent (cc) basis.¹⁴ A regular hexagonal geometry is used for the ground and excited states with experimental C–C and C–H bond lengths of 1.397 and 1.084 Å.¹⁵ The six π electrons are distributed among six π orbitals. These are $a_{2u}(1b_{1u})$, $e_{1g}(1b_{2g})$, $e_{1g}(1b_{3g})$, $e_{2u}(1b_{1u})$, $e_{2u}(1a_u)$, and $b_{2g}(2b_{3g})$ in order of energy in D_{6h} (D_{2h}) symmetry. They are designated by 3, 2, 1, 1', 2' and 3', respectively. The occupied orbitals in the HF approximation are numbered from the highest one down and the unoccupied orbitals from the lowest one up. The orbitals i and i' are called a conjugated pair and the well-known pairing properties^{16,17} are satisfied.

Orthogonal and nonorthogonal orbitals of benzene are given in Fig. 1. The nonorthogonal LMO's were obtained by

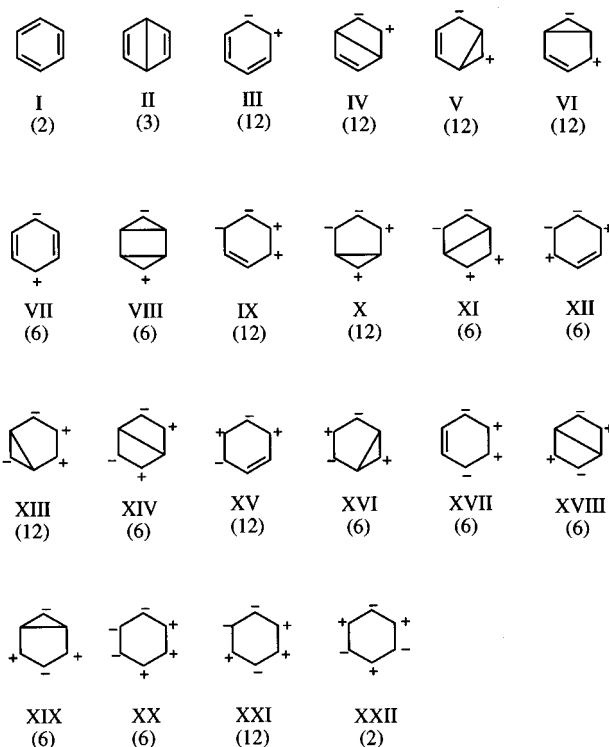


FIG. 2. Rumer diagrams and number of equivalent individual structures for the 1^1A_{1g} symmetry of benzene.

projecting CASSCF MO's onto the free-atom minimum basis set of $2p$ functions of the same cc-VDZ basis. The general contraction scheme is used in Dunning's cc basis set and the minimum basis set of the atomic $2p$ function consists of all the p -type Gaussian primitives. The d polarization functions are not included although they are used for the CASSCF calculations. The nonorthogonal orbital is again well localized on a single carbon atom. As noticed by Ruedenberg,⁸ each nonorthogonal orbital has a very high overlap with the corresponding free-atom $2p$ function, $\langle \lambda_1 | 2p \rangle = 0.9941$ and has a good overlap with its two nearest neighbors, $\langle \lambda_1 | \lambda_2 \rangle = 0.3304$. The two π orbitals in meta and para positions have overlaps of 0.0772 and 0.0335, respectively. Note the shift of the nodal planes on going from orthogonal to nonorthogonal orbitals. We observe that the π orbital becomes slightly inflated due to the relaxation of orthogonality constraints.

In the VB treatment, there are 22 different types of bonding schemes with 175 structures in benzene and these are given in Fig. 2. Each of these bonding schemes gives rise to a linearly independent symmetry function. The number in parentheses in the figure shows the number of equivalent structures with 1^1A_{1g} symmetry. There are five covalent VB structures, two of which are Kekule and three of which are Dewar structures.

In Table I we present the structure occupation numbers for the ground state of benzene. For comparison, previous CASVB results with orthogonal orbitals and SC-VB results by Tantardini *et al.*¹⁸ are also listed in the table. Although the basis set used in the SC-VB is of inferior quality, the

TABLE I. Occupation numbers for $1^1A_{1g}^-$ symmetry structures of benzene.

Symmetry structure	Orthogonal orbitals	Nonorthogonal orbitals	SC-VB with STO basis ^a
I	0.154	0.209	0.222
II	0.076	0.104	0.110
III	0.252	0.246	0.251
IV	0.118	0.108	0.117
V	0.045	0.052	0.042
VI	0.043	0.027	0.038
VII	0.025	0.041	0.023
VIII	0.008	0.008	0.007
IX	0.002	-0.001	0.001
X	0.005	0.002	0.003
XI	0.000	0.000	0.000
XII	0.019	0.008	0.012
XIII	0.004	0.001	0.002
XIV	0.013	0.006	0.009
XV	0.117	0.105	0.086
XVI	0.023	0.022	0.016
XVII	0.018	0.004	0.011
XVIII	0.031	0.024	0.021
XIX	0.022	0.019	0.015
XX	0.000	0.000	0.000
XXI	0.007	0.001	0.003
XXII	0.017	0.014	0.010

^aG. F. Tantardini, M. Raimondi, and M. Simonetta, *J. Am. Chem. Soc.* **99**, 2913 (1977).

comparison is still interesting. We observe that the CASVB results with nonorthogonal orbitals are closer to the SC-VB results than when the orthogonal orbitals are used. It is noted, however, that the variation of occupation numbers on going from orthogonal to nonorthogonal orbitals is not so large, and that it does not change the general trend.

The ground state of benzene is classified as a covalent state in view of the alternant hydrocarbons. Both CASVB descriptions show that the most important contributions come from the two Kekule, three Dewar and 24 orthopolar (an electron is transferred from one orbital to that centered on an adjacent atom) structures. The occupation number of the Dewar structures is about half of that of the Kekule structures. However, the occupation numbers for individual structures imply that the Kekule structure is the most important and that the next most important is the Dewar structure. As noticed by Ohanessian and Hiberty,⁷ the relative weights of the covalent structures increase and those of polar structures decrease with use of the nonorthogonal orbitals. The occupation number formed from five covalent structures yields 0.313 when nonorthogonal orbitals are used while the SC-VB gives 0.332.

The leading VB structures with their structure occupation numbers for the ground and valence $\pi \rightarrow \pi^*$ singlet excited states of benzene are shown in Fig. 3. For comparison, the previous results with orthogonal orbitals are also listed in parentheses.

The excited states of benzene were discussed in detail elsewhere.¹⁷ They may be classified into the covalent minus states and ionic plus states with the use of the alternancy symmetry. The covalent minus states and ionic plus states exhibit different behavior as far as electron correlation is

concerned. In a MO treatment, the electronic excited states are described in terms of singly, doubly, ..., excited configurations constructed from occupied and unoccupied delocalized orbitals. The ionic plus states are dominated by the single excitations but covalent minus states include a large fraction of doubly excited configurations. It is now well-known that dynamic $\sigma-\pi$ polarization effects are significant for the ionic plus states, since π ionic configurations strongly polarize the σ space.

The VB description gives a quite different picture for the excitation from the MO description. The excitation process is represented in VB theory in terms of the rearrangement of spin couplings and charge transfer. The former generates the covalent excited states and the latter gives rise to the ionic excited states, in which the covalent bond is broken and a new ionic bond is formed. Thus, the singly, doubly, ... polar structures are generated from their respective "parent" ground-state covalent (nonpolar), singly, ... polar structures.

The lowest singlet $\pi \rightarrow \pi^*$ excited state is $1^1B_{2u}^-$ ($1^1B_{3u}^-$). The $1^1B_{2u}^-$ state is mainly described by HOMO \rightarrow LUMO configurations of $1 \rightarrow 2'$ and $2 \rightarrow 1'$ in a MO treatment. The $1^1B_{2u}^-$ state is described in a CASVB picture predominantly by a combination of the covalent Kekule and the corresponding orthopolar structures of type III. There are no significant contributions from the Dewar structures or the corresponding orthopolar structures (IV). Although the relative weights change upon going from orthogonal to nonorthogonal orbitals, the general feature is almost invariant.

We observe that linear combinations of the two equivalent Kekule structures generate the plus and minus states. Their positive combination gives rise to the totally symmetric $1^1A_{1g}^-$ ground state, while the negative combination yields the excited $1^1B_{2u}^-$ ($1^1B_{3u}^-$).

The second $\pi \rightarrow \pi^*$ excited state of benzene is $1^1B_{1u}^+$ ($1^1B_{2u}^+$). The state is dominated by singly excited configurations arising from degenerate HOMO \rightarrow LUMO excitations of $1 \rightarrow 1'$ and $2 \rightarrow 2'$ in a MO picture. Thus, the state has an ionic nature. Figure 3 shows that the state is described by a number of ionic structures. There is no contribution from the covalent structures. The leading ionic structures are the doubly polar structures. These structures come from the orthopolar structures of the ground state. Thus, one of the remaining covalent bonds in the VB structures of III is broken, and the plus and minus charges are generated so as to favor the electrostatic interactions as much as possible. The relative weights of the ionic structures in the ground state decrease, as discussed above, when nonorthogonal orbitals are used. Similarly, the relative weights of the doubly polar structures decrease in the $1^1B_{1u}^+$ ($1^1B_{2u}^+$) state. The next most important structures are the orthopolar structures, which originate from the two Kekule structures of the ground state. The parapolar structures must come from the Dewar structures of the ground state. Thus, the relative ratios of the occupation numbers of these three leading polar structures are similar to those of the corresponding parent structures in the ground state.

The third valence excited states are the degenerate $1^1E_{1u}^+$ ($1^1B_{3u}^+$, $2^1B_{2u}^+$) states. The $1^1E_{1u}^+$ ($1^1B_{3u}^+$) state is the plus state

$1^1A_{1g}^- (1^1A_{g^-})$

$$0.2094 \left(\begin{array}{c} 0.1537 \end{array} \right) \left[\text{Benzene} + \text{Benzene} \right] + 0.1045 \left(\begin{array}{c} 0.0757 \end{array} \right) \left[\text{Resonance Structure 1} + \text{Resonance Structure 2} + \text{Resonance Structure 3} \right]$$

$$+ 0.2463 \left(\begin{array}{c} 0.2520 \end{array} \right) \left[\text{Resonance Structure 4} + \text{Resonance Structure 5} + 5 \text{ other pairs of RS} \right]$$

$$+ 0.1076 \left(\begin{array}{c} 0.1179 \end{array} \right) \left[\text{Resonance Structure 6} + \text{Resonance Structure 7} + 5 \text{ other pairs of RS} \right]$$

$$+ 0.1050 \left(\begin{array}{c} 0.1172 \end{array} \right) \left[\text{Resonance Structure 8} + \text{Resonance Structure 9} + 5 \text{ other pairs of RS} \right]$$

+

 $1^1B_{2u}^- (1^1B_{3u}^-)$

$$0.4663 \left(\begin{array}{c} 0.3748 \end{array} \right) \left[\text{Benzene} - \text{Benzene} \right]$$

$$+ 0.4271 \left(\begin{array}{c} 0.4659 \end{array} \right) \left[\text{Resonance Structure 4} - \text{Resonance Structure 5} + 5 \text{ other pairs of RS} \right]$$

$$+ 0.0596 \left(\begin{array}{c} 0.0740 \end{array} \right) \left[\text{Resonance Structure 8} - \text{Resonance Structure 9} + 5 \text{ other pairs of RS} \right]$$

+ ...

 $1^1B_{1u}^+ (1^1B_{2u}^+)$

$$0.3415 \left(\begin{array}{c} 0.3510 \end{array} \right) \left[\text{Resonance Structure 4} - \text{Resonance Structure 5} + 5 \text{ other pairs of RS} \right]$$

$$+ 0.2674 \left(\begin{array}{c} 0.2217 \end{array} \right) \left[\text{Resonance Structure 4} - \text{Resonance Structure 5} + 5 \text{ other pairs of RS} \right]$$

$$+ 0.1463 \left(\begin{array}{c} 0.1342 \end{array} \right) \left[\text{Resonance Structure 6} - \text{Resonance Structure 7} + 2 \text{ other pairs of RS} \right]$$

$$+ 0.0815 \left(\begin{array}{c} 0.0938 \end{array} \right) \left[\text{Resonance Structure 8} - \text{Resonance Structure 9} \right]$$

+

 $1^1E_{1u}^+ (1^1B_{3u}^+)$

$$0.1210 \left(\begin{array}{c} 0.1091 \end{array} \right) \left[\text{Resonance Structure 4} - \text{Resonance Structure 5} + \text{Resonance Structure 6} - \text{Resonance Structure 7} \right]$$

$$+ 0.1175 \left(\begin{array}{c} 0.0951 \end{array} \right) \left[\text{Resonance Structure 4} - \text{Resonance Structure 5} + \text{Resonance Structure 6} - \text{Resonance Structure 7} \right]$$

$$+ 0.1013 \left(\begin{array}{c} 0.0811 \end{array} \right) \left[\text{Resonance Structure 4} + \text{Resonance Structure 5} - \text{Resonance Structure 6} + \text{Resonance Structure 7} \right]$$

$$+ 0.0998 \left(\begin{array}{c} 0.0913 \end{array} \right) \left[\text{Resonance Structure 6} - \text{Resonance Structure 7} + \text{Resonance Structure 8} - \text{Resonance Structure 9} \right]$$

$$+ 0.0794 \left(\begin{array}{c} 0.0784 \end{array} \right) \left[\text{Resonance Structure 6} - \text{Resonance Structure 7} + \text{Resonance Structure 8} - \text{Resonance Structure 9} \right] + ..$$

 $1^1E_{1u}^+ (2^1B_{2u}^+)$

$$0.1457 \left(\begin{array}{c} 0.1173 \end{array} \right) \left[\text{Resonance Structure 4} - \text{Resonance Structure 5} + \text{Resonance Structure 6} - \text{Resonance Structure 7} \right]$$

$$+ 0.0807 \left(\begin{array}{c} 0.0727 \end{array} \right) \left[\text{Resonance Structure 4} - \text{Resonance Structure 5} \right]$$

$$+ 0.0756 \left(\begin{array}{c} 0.0685 \end{array} \right) \left[\text{Resonance Structure 6} - \text{Resonance Structure 7} + \text{Resonance Structure 8} - \text{Resonance Structure 9} \right]$$

$$+ 0.0741 \left(\begin{array}{c} 0.0684 \end{array} \right) \left[\text{Resonance Structure 4} - \text{Resonance Structure 5} + \text{Resonance Structure 6} - \text{Resonance Structure 7} \right]$$

$$+ 0.0679 \left(\begin{array}{c} 0.0711 \end{array} \right) \left[\text{Resonance Structure 4} - \text{Resonance Structure 5} + \text{Resonance Structure 6} - \text{Resonance Structure 7} \right]$$

$$+ 0.0678 \left(\begin{array}{c} 0.0547 \end{array} \right) \left[\text{Resonance Structure 6} - \text{Resonance Structure 7} - \text{Resonance Structure 8} + \text{Resonance Structure 9} \right] + ..$$

 $1^1E_{2g}^- (2^1A_g^-)$

$$0.5011 \left(\begin{array}{c} 0.4285 \end{array} \right) \left[\text{Resonance Structure 1} - 0.5 \text{Resonance Structure 2} - 0.5 \text{Resonance Structure 3} \right]$$

$$+ 0.2382 \left(\begin{array}{c} 0.2687 \end{array} \right) \left[\text{Resonance Structure 4} + \text{Resonance Structure 5} + \text{Resonance Structure 6} + \text{Resonance Structure 7} \right]$$

$$+ 0.0789 \left(\begin{array}{c} 0.0879 \end{array} \right) \left[\text{Resonance Structure 6} - \text{Resonance Structure 7} - \text{Resonance Structure 8} - \text{Resonance Structure 9} \right]$$

+ ...

 $1^1E_{2g}^- (1^1B_{1g}^-)$

$$0.5011 \left(\begin{array}{c} 0.4285 \end{array} \right) \left[\text{Resonance Structure 1} - \text{Resonance Structure 2} \right]$$

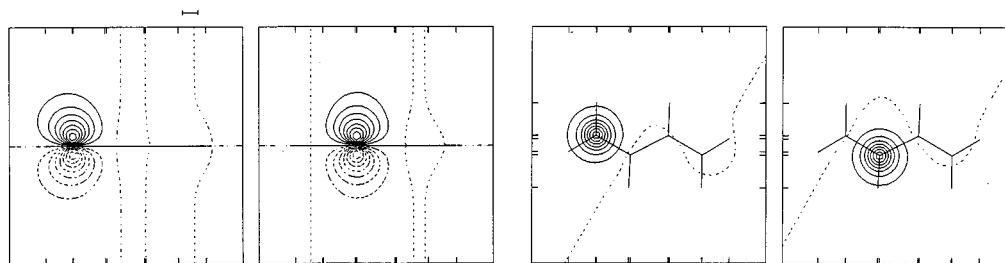
$$+ 0.1971 \left(\begin{array}{c} 0.2214 \end{array} \right) \left[\text{Resonance Structure 4} + \text{Resonance Structure 5} - \text{Resonance Structure 6} - \text{Resonance Structure 7} \right]$$

$$+ 0.1611 \left(\begin{array}{c} 0.1824 \end{array} \right) \left[\text{Resonance Structure 4} + \text{Resonance Structure 5} - \text{Resonance Structure 6} - \text{Resonance Structure 7} \right]$$

+ ...

FIG. 3. Description of the ground and excited state CASVB wave functions of benzene with nonorthogonal orbitals. Values are the occupation numbers of the Rumer functions. RS indicates the corresponding symmetry related resonance structures. Values in parentheses are the occupation numbers of CASVB description with orthogonal orbitals.

Orthogonal orbitals



Non-orthogonal orbitals

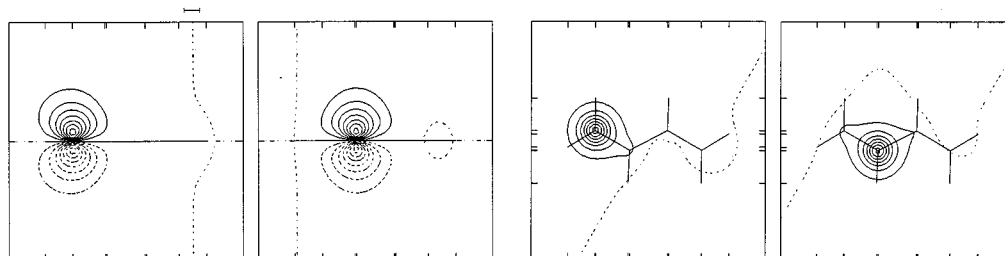


FIG. 4. Orthogonal and nonorthogonal π orbitals of *trans*-butadiene. Contours are plotted in a σ_h mirror (perpendicular to the molecular plane) and plotted in the plane 0.3 Å above the σ_h plane.

corresponding to the minus ${}^1B_{2u}^-$ (${}^1B_{3u}^-$) state. The CASSCF wave function for the ${}^1E_{1u}^+$ (${}^1B_{3u}^+$) is dominated by the singly excited configurations $1 \rightarrow 2'$ and $2 \rightarrow 1'$ and the ${}^1E_{1u}^+$ ($2{}^1B_{2u}^+$) state is dominated by the singly excited configurations of $1 \rightarrow 1'$ and $2 \rightarrow 2'$. These states are ionic in nature. The ionic character of these states can easily be found from a CASVB description.

The highest valence excited states treated here are the covalent ${}^1E_{2g}^-$ (${}^1A_g^-$, ${}^1B_{1g}^-$). The CASSCF ${}^1E_{2g}^-$ (${}^1A_g^-$) wave function is a mixture of configurations $1 \rightarrow 3'$ and $3 \rightarrow 1'$ but includes a large fraction of the doubly excited configurations $(1)^2 \rightarrow (1')^2$, $1 \rightarrow 2'$, $2 \rightarrow 1'$, ..., etc. The ${}^1E_{2g}^-$ (${}^1B_{1g}^-$) state is also represented by a mixture of configurations $2 \rightarrow 3'$ and $3 \rightarrow 2'$ and doubly excited configurations. The states have a predominantly Dewar character with smaller contributions from the corresponding orthopolar VB structures IV. No contribution can be found from the Kekule structures. Thus, the Kekule structures dominate the ground state and the singly excited ${}^1B_{2u}^-$ (${}^1B_{3u}^-$) state while the Dewar structures dominate the doubly excited degenerate ${}^1E_{2g}^-$ states.

B. Butadiene

CASSCF functions were computed with an active space of 4 π electrons in 4 π orbitals. The calculations were done using the experimental geometry¹⁹ with the $(3s2p1d/2s)$ basis.¹⁴ The orthogonal and nonorthogonal π LMO's of *trans*-butadiene are shown in Fig. 4. The nonorthogonal π LMO's were constructed by the method outlined in the case of benzene. The π LMO's are well localized on a single atomic center with small localization tails onto the neighboring carbons. Each π LMO again resembles an atomiclike $2p$ function. The overlap between the terminal (center) π LMO

and an atomic $2p$ of the free atom is 0.9912 (0.9883). The overlaps between LMO's are listed in Table II.

The occupation numbers for *trans*-butadiene are summarized in Table III. The ground state is mainly comprised of the Kekule-type structure with a small contribution from the Dewar-type structure, while the doubly excited covalent $2{}^1A_g^-$ state is expressed predominantly by a Dewar-type structure with small mixing from the Kekule-type structure. MRMP predicts that the transition occurs at 6.31 eV above the ground state.²⁰ Again, we can see from Table III that CASVB with nonorthogonal orbitals makes the weights of the covalent structures increase relative to those of the ionic structures. However, the effect of orbital relaxation is not so significant.

The dipole-allowed $1{}^1B_u^+$ state is well described by a singly excited $\pi \rightarrow \pi^*$ configuration, HOMO \rightarrow LUMO in a MO description. MRMP places the energy of the $1{}^1B_u^+$ state at 6.21 eV (Ref. 20) above the ground state or 0.3 eV above the experimental intensity maximum of 5.92 eV. The state has an ionic nature which can be readily interpreted in terms of the VB resonance structures. The $1{}^1B_u^+$ state is a mixture of a large number of ionic structures. The covalent structures

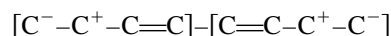
TABLE II. Overlap integrals between the nonorthogonal p orbitals of butadiene.

	λ_1	λ_2	λ_3	λ_4
λ_1	1.0			
λ_2	0.3635	1.0		
λ_3	0.0633	0.3104	1.0	
λ_4	0.0083	0.0633	0.3635	1.0

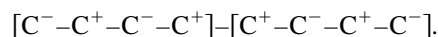
TABLE III. The occupation numbers of the ground and excited state CASVB wave functions of butadiene.

Structure	Occupation numbers	
	Orthogonal MO	Nonorthogonal MO
$1^1A_g^-$ (ground state)		
$[C=C-C=C]$	0.3960	0.4789
$[C-C=C-C]$	0.0525	0.0633
$[C^-C^+C=C]+[C=C-C^+C^-]$	0.1970	0.1746
$[C^+C^-C=C]+[C=C-C^-C^+]$	0.1812	0.1565
$[C-C^+C^-C]+[C-C^-C^+C]$	0.0436	0.0312
$[C^-C-C^+C]+[C-C^-C-C^+]$	0.0194	0.0185
$[C^+C-C^-C]+[C-C^+C-C^-]$	0.0152	0.0126
$[C^-C=C-C^+]+[C^+C=C-C^-]$	0.0102	0.0102
$[C^-C^+C^-C^+]+[C^+C^-C^+C^-]$	0.0506	0.0369
$[C^-C^+C^+C^-]$	0.0182	0.0100
$[C^+C^-C^-C^+]$	0.0155	0.0078
$[C^-C^-C^+C^+]+[C^+C^+C^-C^-]$	0.0002	-0.0002
$2^1A_g^-$ (covalent)		
$[C-C=C-C]$	0.6059	0.6439
$[C=C-C=C]$	0.0789	0.0809
$[C-C^-C^+C]+[C-C^+C^-C]$	0.2330	0.1967
$[C^+C-C^-C]+[C-C^-C-C^+]$	0.0219	0.0249
$[C^-C-C^+C]+[C-C^+C-C^-]$	0.0118	0.0166
$[C^-C^+C=C]+[C=C-C^+C^-]$	0.0188	0.0169
$[C^+C^-C=C]+[C=C-C^-C^+]$	0.0154	0.0142
$[C-C=C-C^+]+[C^+C=C-C^-]$	0.0040	0.0040
$[C^+C^-C^-C^+]$	0.0037	0.0026
$[C^-C^+C^+C^-]$	0.0028	0.0017
$[C^-C^+C^-C^+]+[C^+C^-C^+C^-]$	0.0038	0.0024
$[C^-C^-C^+C^+]+[C^+C^+C^-C^-]$	0.0002	0.0000
$1^1B_u^+$ (ionic)		
$[C^-C^+C=C]-[C=C-C^+C^-]$	0.1940	0.2157
$[C^+C^-C=C]-[C=C-C^-C^+]$	0.1488	0.1655
$[C^-C=C-C^+]-[C^+C=C-C^-]$	0.1362	0.1367
$[C^-C-C^+C]-[C-C^+C-C^-]$	0.1322	0.1278
$[C^+C-C^-C]-[C-C^-C-C^+]$	0.1006	0.0942
$[C^-C^-C^+C]-[C-C^+C^-C]$	0.0948	0.1038
$[C^-C^+C^-C^+]-[C^+C^-C^+C^-]$	0.1900	0.1576
$[C^-C^-C^+C^+]-[C^+C^+C^-C^-]$	0.0034	-0.0014

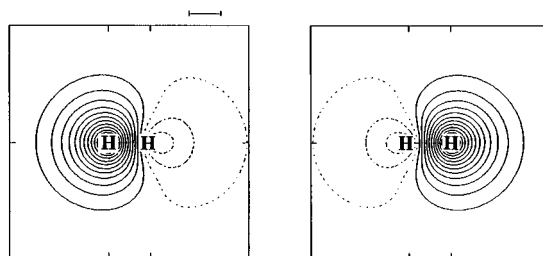
are strictly excluded from the ionic states. The leading terms are the singly and doubly polar structures,



and



Orthogonal orbitals



Non-orthogonal orbitals

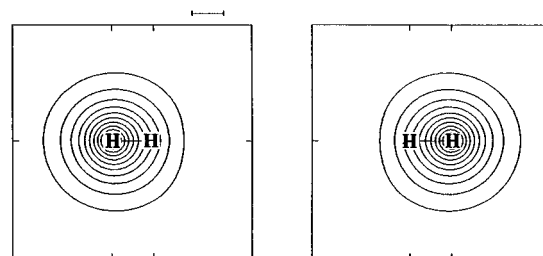


FIG. 5. Orthogonal and nonorthogonal $1s$ orbitals of the hydrogen molecule.

Although singly and doubly ionic structures have nearly the same occupation numbers when orthogonal orbitals are used, use of nonorthogonal orbitals enhances the weight of singly ionic structures and diminishes the weight of more polar doubly ionic structures.

C. Hydrogen molecule

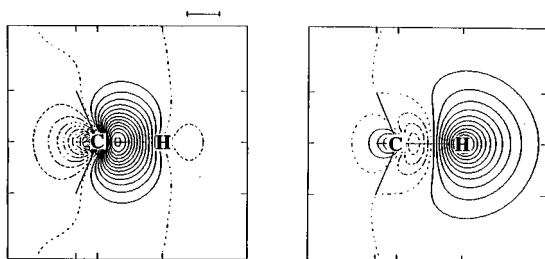
The first quantum mechanical treatment of the hydrogen molecule was done by Heitler and London in 1927.²¹ Their ideas have been extended to give a general theory of chemical bonding, the VB theory. It is of interest to consider the problem using the present modern CASVB approach. The basis set used is of double-zeta plus polarization quality. Orthogonal and nonorthogonal orbitals of H_2 at 0.7 Å are shown in Fig. 5. Nonorthogonal orbitals were obtained by projecting the CASSCF MO's onto the $1s$ atomic function of the free atom. We observe that the orthogonal LMO is deformed significantly from the atomic $1s$ function and has a small tail on the other hydrogen atom due to the orthogonality constraint. The orthogonality requirement between LMO's forces small antibonding admixture from orbitals on neighboring atoms into each LMO. On the contrary, the nonorthogonal LMO looks very much like an atomic $1s$ function (the overlap is 0.9859) and the LMO's overlap strongly with each other (0.7775).

The occupation numbers of covalent and ionic structures in the CASVB description in terms of orthogonal LMO's are

$$0.6082[H_A-H_B]+0.3918\{[H_A^+H_B^-]+[H_A^-H_B^+]\}.$$

Nonorthogonal LMO's change the picture of ionic-covalent resonance dramatically,

Orthogonal orbitals



Non-orthogonal orbitals

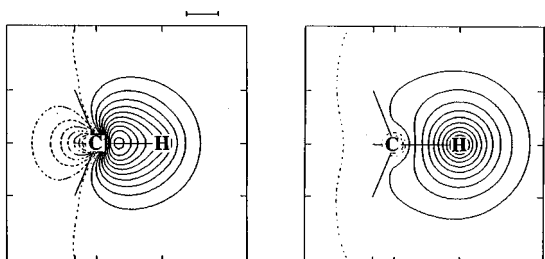


FIG. 6. A pair of orthogonal and nonorthogonal carbon sp^3 and hydrogen $1s$ orbitals of methane.

$$0.9896[H_A - H_B] + 0.0104\{[H_A^+ H_B^-] + [H_A^- H_B^+]\}.$$

Orbital relaxation increases the covalent character of the H–H bond and decreases the ionic character. This trend is stronger than that observed in the case of π bonds. The present description seems more reasonable conceptually.

D. Methane

Methane is also a molecule to which CASVB theory with orthogonal orbitals was applied. With orthogonal orbitals CASVB resembles Pauling's pioneering view²² that each of the four equivalent covalent bonds is taken to arise from the overlap of a $1s$ function on a hydrogen atom and one of four orthogonal sp^3 hybrids on carbon, with singlet coupling of the associated electron pairs. However, there are also important differences. One of them is that CASVB with orthogonal orbitals needs large numbers of ionic structures. The occupation number of a totally symmetric covalent perfect pairing structure is only 0.1021.

A tetrahedral geometry with a CH bond length equal to 1.091 Å was used. The basis set used is the double-zeta plus polarization, ($3s2p1d/2s1p$) taken from Dunning's cc-pVDZ.¹⁴ With the restriction that the $1s$ orbital of carbon remains doubly occupied, the eight valence electrons are treated as active electrons and distributed among eight valence orbitals ($2a_1$, $1t_2$, $2t_2$, and $3a_1$). The sp^3 -like hybrid atomic orbitals were used as basis AO's for carbon instead of the free-atomic $2s$ and $2p$ functions. Hybrid orbitals were determined by Boys' localization procedure, mixing carbon $2s$ and three $2p$ AO's. Hydrogen LMO's were computed by projecting CASSCF MO's onto the corresponding SCF $1s$

TABLE IV. Overlap integrals between the nonorthogonal orbitals of methane.^a

	λ_C	λ_H	$\lambda_{C'}$	$\lambda_{H'}$
λ_C	1.0			
λ_H	0.7498	1.0		
$\lambda_{C'}$	0.0090	0.1359	1.0	
$\lambda_{H'}$	0.1359	0.2694	0.7498	1.0

^aThe λ_C and λ_H denote the carbon sp^3 -like hybrid and hydrogen $1s$ orbitals, respectively.

functions. The projected localization procedure yields four equivalent pairs of LMO's. A pair of these LMO's is shown in Fig. 6. Each pair comprises an orbital predominantly localized on the carbon and a second orbital predominantly localized on the hydrogen. Their overlap integrals with the corresponding carbon hybrid AO and hydrogen $1s$ AO are found to be $\langle \lambda_C | sp^3 \rangle = 0.9787$ and $\langle \lambda_H | 1s \rangle = 0.9880$, respectively. The overlaps between LMO's are given in Table IV. Contrary to the assumption of classical VB theory introduced by Pauling, two sp^3 -like hybrids are not strictly orthogonal but have a small overlap of 0.0090. However, each of these hybrid orbitals overlaps most strongly (0.7498) with one slightly deformed hydrogen $1s$ orbital to which it points. Comparison of orthogonal and nonorthogonal orbitals shows that the orthogonality restriction has rather significant effects on each orbital. The carbon sp^3 -like hybrid and hydrogen $1s$ orbitals relax substantially on going from the orthogonal to nonorthogonal orbitals.

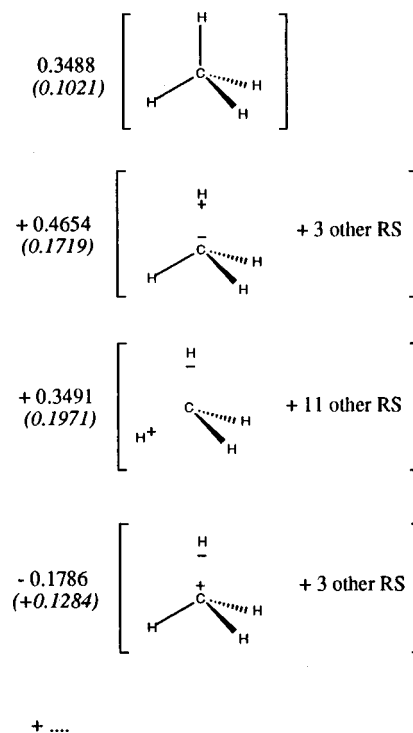


FIG. 7. Description of the CASVB wave function of the ground state methane with nonorthogonal orbitals. RS indicates the corresponding symmetry related resonance structures. Values in parentheses are the occupation numbers of the CASVB description with orthogonal orbitals.

The number of linearly independent symmetry structures belonging to the A_1 irreducible representation of the T_d point group is 104 for methane. The important VB structures and their occupation numbers are given in Fig. 7. We arranged the VB structures in the order of decreasing occupation number for individual structures. Both CASVB methods with orthogonal and nonorthogonal orbitals give a similar general conceptual picture, but the variation in the relative weight of each structure is rather significant. The most important structure is one with four covalent bonds, with the occupation number of 0.3488. This is three times larger than that of orthogonal CASVB. Next are VB structures with three covalent bonds and one ionic bond, with carbon negative. Then follow the structures with two covalent bonds and two ionic bonds. Note that the sum of the occupation numbers from the first three structures exceeds 1.0. The next contributions are from VB structures with three covalent bonds and one ionic bond with carbon positive.

The feature that a structure with carbon negative is better (larger occupation number) than carbon positive is consistent with the result $\mu(r_e) > 0$ for the CH bond electric dipole moment obtained from the analysis of FIR spectroscopy and quantum Monte Carlo calculations of deuterated methanes.²³ Although we omit the details, we also confirmed that a structure with Si positive is better than Si negative in SiH_4 . This can be compared to the result $\mu(r_e) < 0$ for the SiH bond dipole moment obtained from the analysis of microwave spectra of deuterated silanes.²⁴

The occupation number for structures containing positive carbon is calculated to be negative. This somewhat unfavorable result may arise from the definition of the occupation numbers.

IV. SUMMARY

Chemists are familiar with localized orbitals and the classical VB resonance concepts. The canonical MO method puts electrons into orthogonal delocalized MO's while the VB method puts electrons into nonorthogonal AO's. The mathematical drawbacks of VB theory and its difficulties with magnetic properties and spectra led to an emphasis on the MO method. For quantitative calculations, the MO method has greatly overshadowed the VB method, sacrificing the intuitive advantages of pictorial concepts for the conveniences of symmetry. As shown in this paper and in previous papers by Ruedenberg⁸ and by McDouall and Robb¹¹ one can easily obtain a VB-type wave function simply by transforming a canonical CASSCF function without any loss in accuracy.

Any full CI wave function is invariant under linear transformations of the defining orbitals. The present study exploits it to suggest an alternative representation of the CASSCF wave function. Nonorthogonal orbitals were constructed so as to have maximal overlaps with the corresponding minimal basis set of the AO's of the free atoms. These nonorthogonal MO's are equivalent to the atom-adapted FORS MO's defined by Ruedenberg.⁸ The VB structures

which are composed of such nonorthogonal atomiclike MO's constitute the wave function closest to the concept of the oldest and most simple VB method. Use of nonorthogonal orbitals places a higher weight on covalent structures than when orthogonal orbitals are used. The results demonstrate the validity of the CASVB method as a powerful tool for describing the various electronic structures of molecules.

ACKNOWLEDGMENTS

The authors thank Professor Mark S. Gordon (Iowa State University) for valuable discussions. The present research is supported in part by a Grant-in-Aid for scientific research from the Ministry of Education, Science, and Culture of Japan. One of the authors (K.H.) also thanks a grant by Kawasaki Steel 21st Century Foundation. The computations were carried out on the IBM RS6000-591 workstations. The CASSCF/CASVB wave functions were obtained by a modified version of HONDO96 (Ref. 25). Orbital contour maps were plotted using GAMESS program (Ref. 26).

- ¹K. Hirao, H. Nakano, K. Nakayama, and M. Dupuis, *J. Chem. Phys.* **105**, 9227 (1996).
- ²P. E. Siegbahn, A. Heiberg, B. O. Roos, and B. Levy, *Phys. Scr.* **21**, 323 (1980); B. O. Roos, P. R. Taylor, and P. E. Siegbahn, *Chem. Phys.* **48**, 157 (1980); B. O. Roos, *Int. J. Quantum Chem.* **S14**, 175 (1980).
- ³K. Ruedenberg and K. R. Sundberg, in *Quantum Science*, edited by J. L. Calais, O. Goscinski, J. Linderberg, and Y. Ohrn (Plenum, New York, 1976), p. 505; L. M. Cheung, K. R. Sundberg, and K. Ruedenberg, *Int. J. Quantum Chem.* **16**, 1103 (1979).
- ⁴K. Andersson, P. Malmqvist, B. O. Roos, A. J. Sadlej, and K. Wolinski, *J. Phys. Chem.* **94**, 5483 (1990); K. Andersson, P. Malmqvist, and B. O. Roos, *J. Chem. Phys.* **96**, 1218 (1992).
- ⁵K. Hirao, *Chem. Phys. Lett.* **190**, 374 (1992); **196**, 397 (1992); **201**, 59 (1993); *Int. J. Quantum Chem.* **S26**, 517 (1992).
- ⁶J. M. Foster and S. F. Boys, *Rev. Mod. Phys.* **32**, 300 (1960).
- ⁷G. Ohanessian and P. C. Hiberty, *Chem. Phys. Lett.* **137**, 437 (1987).
- ⁸K. Ruedenberg, M. W. Schmidt, M. M. Gilbert, and S. T. Elbert, *Chem. Phys.* **71**, 41,51,65 (1982).
- ⁹J. J. W. McDouall and M. A. Robb, *Chem. Phys. Lett.* **132**, 319 (1986).
- ¹⁰C. Edmiston and K. Ruedenberg, *Rev. Mod. Phys.* **53**, 457 (1965).
- ¹¹J. J. W. McDouall and M. A. Robb, *Chem. Phys. Lett.* **142**, 131 (1987).
- ¹²D. L. Cooper, J. Gerratt, and M. Raimondi, *Nature (London)* **323**, 699 (1986); *Adv. Chem. Phys.* **27** (Part II), 319 (1987).
- ¹³T. Thorsteinsson, D. L. Cooper, J. Gerratt, P. B. Karadakov, and M. Raimondi, *Theor. Chim. Acta* **93**, 343 (1996).
- ¹⁴T. H. Dunning, *J. Chem. Phys.* **90**, 1007 (1989).
- ¹⁵A. Langseth and B. P. Stoicheff, *Can. J. Phys.* **34**, 350 (1956).
- ¹⁶R. Pariser, *J. Chem. Phys.* **24**, 250 (1956).
- ¹⁷T. Hashimoto, H. Nakano, and K. Hirao, *J. Chem. Phys.* **104**, 6244 (1996).
- ¹⁸G. F. Tantardini, M. Raimondi, and M. Simonetta, *J. Am. Chem. Soc.* **99**, 2913 (1977).
- ¹⁹W. Haugen and M. Traetteberg, *Acta Chem. Scand.* **20**, 1726 (1966).
- ²⁰K. Nakayama, H. Nakano, and K. Hirao, *Int. J. Quantum Chem.* (in press).
- ²¹W. Heitler and F. London, *Z. Phys.* **44**, 455 (1927).
- ²²L. Pauling, *J. Am. Chem. Soc.* **53**, 1367 (1931).
- ²³R. Signorelli, R. Marquardt, M. Quack, and M. A. Suhm, *Mol. Phys.* **89**, 297 (1996).
- ²⁴K. Ohno, H. Matsuura, Y. Endo, and E. Hirota, *J. Mol. Spectrosc.* **111**, 73 (1985).
- ²⁵M. Dupuis, S. Chin, and A. Marquez, in *Relativistic And Electron Correlation Effects in Molecules And Clusters*, NATO ASI Series, edited by G. L. Malli (Plenum, New York, 1992).
- ²⁶M. W. Schmidt, K. K. Baldrige, J. A. Boatz, S. T. Elbert, M. S. Gordon, J. H. Jensen, S. Koseki, N. Matsunaga, K. A. Nguyen, S. Su, T. L. Windus, M. Dupuis, and J. A. Montgomery, *J. Comput. Chem.* **14**, 1347 (1993).